PZT ACTUATED MICROMIRROR FOR NANO-TRACKING OF LASER BEAM FOR HIGH-DENSITY OPTICAL DATA STORAGE

Youngjoo Yee*, Hyo-Jin Nam, See-Hyung Lee, Jong Uk Bu, Young-Sam Jeon, and Seong-Moon Cho

Devices and Materials Lab., LG Corporate Institute of Technology
16 Woomyeon-Dong, Seocho-Ku, Seoul 137-724, Korea
*Phone: +82-2-526-4504, Fax.: +82-2-3461-3508, E-mail: yjyee@lgcit.com

ABSTRACT

A micromirror actuated by piezoelectric cantilevers is proposed as a fine-tracking device for high-density optical data storage. Metal/PZT/metal thin film actuators translate an integrated micromirror along the out-of-plane vertical direction. The parallel motion of the micromirror steers linearly the optical path of the reflected laser beam. Numerical analysis shows that the actuated micromirror can satisfy the tracking speed imposed by the requirement on the access time for the high-density optical data storage up to few tens Gbit/in^2. In this paper, preliminary characteristics of the micromachined PZT actuated micromirror (PAM) are reported. The design and the fabrication process of the PZT actuated micromirror are described. Only a 3600Å-thick PZT film deposited by sol-gel process shows both good electrical and mechanical characteristics for the actuators. The micromirror can be easily actuated up to several micrometers under low voltage operation condition.

INTRODUCTION

Recently, several approaches for high-density data storage are widely investigated based on MEMS technologies. Modified AFM [1], SNOM probe [2], and SIL [3] are good examples of state-of-the art researches. However, these approaches have been focused on the bit size less than 100 nm. In conventional far-field optical data storage such as compact disk (CD) or digital versatile disk (DVD), physical limitation on the legible bit size is determined by the diffraction limit of the pickup optics. The probe beam size limited by the diffraction of the pickup laser can be overcome by optical near-field technique [4] and the recorded bit dimension in optical media can be further reduced using super resolution techniques in magneto optical recording materials [5].

However, it is another critical requirement to control the position of the pickup probe well below the track pitch of the high-density data storage. Due to the inherent properties of MEMS device including accurate actuation and fast response as well as light mass and small volume, micromachined actuators have been studied to be used as fine tracking mechanisms of the magnetic hard disk drive [6]. Optical pickup has potential merit over the other pickup methods in tracking speed because it is basically non-contact system. Considering the tracking speed and the power consumption, it will be more efficient to steer the pickup laser beam trace itself rather than actuating the whole optics module.

In this presentation, an actuated micromirror is proposed as a fine tracking mechanism for the high-density optical data storage as in Figure 1. The actuated micromirror module is assembled with coarse positioning actuator to track the entire optical disk as in Figure 1(a), it provides fine positioning of the laser beam between the data tracks having less than 200-nm pitch. A schematic cross-section of the fine tracking and optical pickup module marked by a circle in (a) is shown in (b). A PZT actuated micromirror (PAM) placed on a 45° submount constructs the fine tracking mechanism marked as a circle in (b). Actuated micromirror alters the ray trace of the laser beam and the beam seeks the nano-scale data passing the focusing optics such as near-field optics. Near-field gap can be maintained by flying head technique using air-bearing surface formed at the bottom surface of the pickup head.

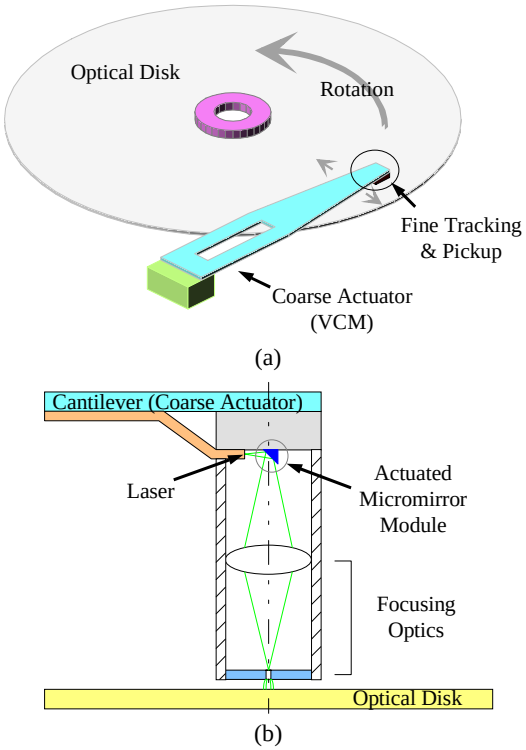

Figure 1: System schematic of the high-density optical data storage using the actuated micromirror as a fine tracking device.

OPERATION PRINCIPLE

Actuated micromirrors were reported as beam scanners [7] and projection display device. However, the actuation accuracy of them is not enough to use for fine positioning of the beam spot with far less than the inter-track dimension of the high-density optical data storage because they operate in torsion mode. In addition, the operation voltage of the electrostatic actuator used in those examples is still too high to be embedded in practical use. Vertical translational motion of the mirror plate is expected to have better steering accuracy than tilting motion in case that the surface to be scanned is far enough from the reflecting mirror surface.

Figure 2 shows an optical system diagram of the pickup using the PZT actuated micromirror (PAM). The out-of-plane translational actuation of the micromirror steers the focused beam spot on the optical disk. Reflected optical signal from the steered position enters into the photodetector through the same optics to read the stored bit. The device structure of the PAM is illustrated in Figure 3 and Figure 4, respectively. Four identical cantilevers located symmetrically around the mirror periphery suspend a gold-coated micromirror plate. Four narrow hinges link each side of the mirror plate and the corresponding cantilevers. The basic frame structure of both the gold mirror and the PZT unimorph actuators is constructed from 2μm-thick low-stress silicon nitride.

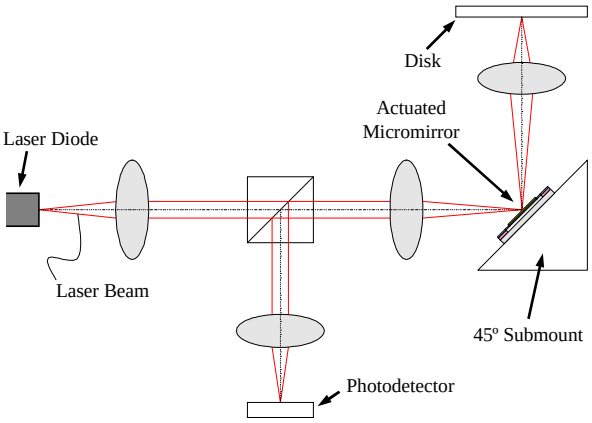

Figure 2: Optical system diagram of high-density data storage pickup using PZT actuated micromirror.

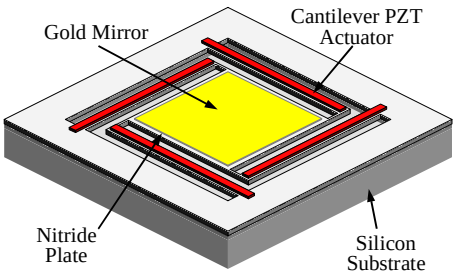

Figure 3: Three-dimensional schematic of the PZT actuated micromirror for nano-steering of the laser beam.

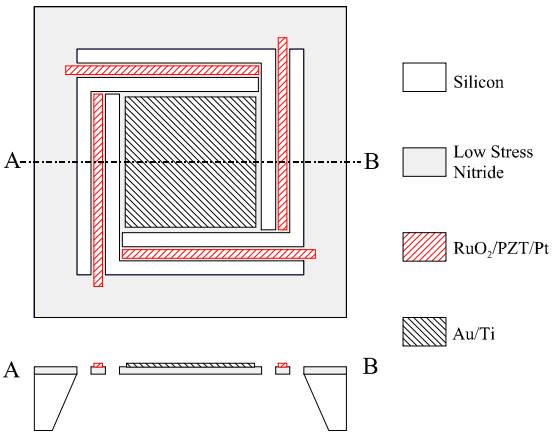

Figure 4: Plain and cross-sectional device structure of the PZT actuated micromirror.

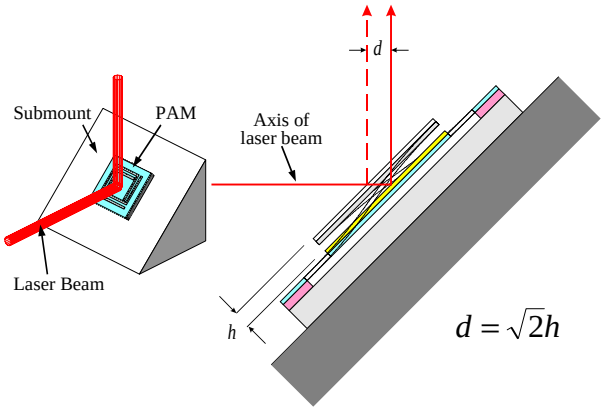

Figure 5: The principle of steering the laser beam by the PZT actuated micromirror (PAM).

The PZT unimorph has a metal/PZT/metal sandwich structure stacked on the low-stress nitride cantilever. Voltage bias applied between the two metal electrodes makes upward bending of the cantilever due to the piezoelectric effect. Bending of each cantilever PZT unimorph is translated into the out-of-plane vertical displacement of the micromirror. The PZT unimorph cantilever can provide large displacement at the free end under a low operating voltage, because small change in stress gradient along the vertical direction results in large deflection of the cantilever [8]. The actuation with low-voltage could be one of the merits in using the PAM. Figure 5 shows the operation principle of the PAM as a fine-tracking mechanism for optical data storage systems by the linear steering of the laser beam. The displacement h of the actuated mirror steers the laser beam as d.

DESIGN AND SIMULATION

The length of each side of the mirror plate was split into 250 μm, 500 μm, and 1000 μm, respectively. The width of hinges is designed to be 10 μm. Suspended micromirror is separated from the square-shaped silicon rim as far as 100 μm. The bulk micromachined silicon rim

serves as an anchor for the cantilevers. The width of the nitride cantilevers is 50 μm and the length depends on the mirror dimension. For example, 250 × 250 μm^2 micromirror has four identical 230 μm-long cantilevers and for a 500 × 500 μm^2 mirror, that of the cantilevers is 355 μm-long, respectively. The residual stress of the 2 μm-thick supporting low-stress nitride layer is designed to be mild tensile of lower than 30 MPa. The thickness of the PZT layer is 3600Å. Thin gold layer is selected as a high reflective mirror surface because it shows the highest reflectivity among several metals compatible with micromachining process [9]. It is very critical which material is used as electrode of the PZT unimorph due to the constraints on the leakage current, the adhesion with the PZT, and the residual stress. In this work, platinum and ruthenium oxide (RuO_2) are selected as the bottom and the top electrode. The thickness of the electrodes should be as thin as possible to reduce the undesirable effects on the mechanical properties of the cantilevers or the residual stress of them should be controlled low enough.

A series of FEM simulations was performed on the mechanical characteristics of the PAM. At first mode resonance of the PAM, the micromirror moves parallel up and down as in Figure 6(a). The resonance frequencies of the PAMs having different mirror size are listed in Table 1. The stress distribution during actuation shows that the highest stress is concentrated on the linkage parts between the hinges and the mirror plate as revealed in Figure 6(b). However, no significant change in stress level is found in most area of the micromirror if the non-uniform stress is not initially built up in micromirror itself. Figure 7 shows the shape of the PAM during operation. From this simulation, it is expected for the micromirror to maintain its initial shape during actuation. From the simulation results, it is clearly predicted that the PAM could steer the incident laser beam without significant distortion in the beam shape. Furthermore, the calculated resonance frequency is high enough to satisfy the servo bandwidth determined by the data access time needed for the high-density optical data storage systems.

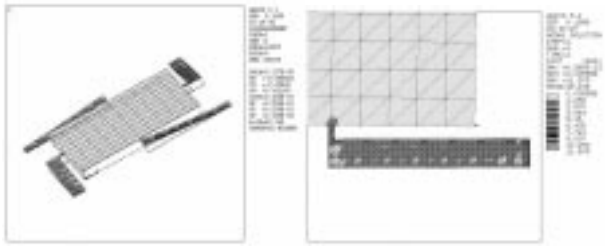

(a) (b)

Figure 6: FEM simulation results by ANSYS. (a) First mode resonance of PAM. (b) Stress distribution during actuation of PAM.

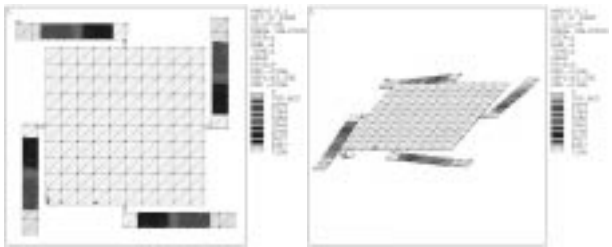

(a) (b)

Figure 7: The shape of the micromirror and suspension cantilevers during actuation. Plain (a) and Three-dimensional view (b).

Table 1: Simulated resonance frequency of PAM

Mirror Size (μm^2)	First mode Resonance (kHz)	Second mode Resonance (kHz)
250 × 250	33.3	54.1
500 × 500	10.1	16.4
1000 × 1000	2.43	3.94

FABRICATION

Metal/PZT/metal Capacitor

In this work, the PZT film was prepared by sol-gel method. Platinum film deposited by sputtering in ultra-high vacuum is chosen as the bottom electrode. The PZT layer was formed by multiple spin coating and thermal curing processes. After four times coating and baking steps, the film was annealed for one minute at 650• by rapid thermal process. The resulting thickness of the PZT film was 3600Å and its composition showed near a morphotropic phase boundary. As the top electrode of the PZT capacitor, ruthenium oxide was deposited by reactive sputtering at 300• . The adhesion of the top electrode is one of the important considerations in actuator applications because the stacked PZT capacitor deforms continuously during actuation. After stacking the whole films, capacitor patterns were delineated by self-align method. The top electrode and the PZT layer were etched sequentially with a common masking layer followed by patterning of the bottom platinum electrode using the other masking step. All of the etching process was carried out using inductively coupled plasma RIE. In the fabrication of the PAM, the etching process requires high selectivity between each layer of the stacked materials because the remaining surface of the silicon nitride layer should be smooth enough to be used as mirror surface. The PZT capacitors were etched using metal mask instead of photoresist for high selectivity [10] and the bottom electrodes were etched with Cl_2/O_2 gas chemistry. The etch rate of the nitride was very low in Cl_2/O_2 based plasma and the good mirror surface could be obtained.

The PZT capacitors were annealed to remove the damages during the dry etching steps. Annealing at 650• for one minute effectively recovers the degradation of the PZT layer during the previous steps as clearly shown in Figure 8. The radiation and charging damages during the dry etching steps resulted in considerable shift toward negative bias in P-E hysteresis curve and

the leakage current was found to be above 10^{-4} A/cm^2 at 10 V bias. The symmetry of the polarization characteristic is recovered and the PZT capacitor shows very stable P-E hysteresis curve even at 20 V bias condition after the thermal annealing as in Figure 9. The leakage current is also drastically reduced under 10^{-6} A/cm^2 level at 10 V bias as shown in Figure 10. Annealed PZT capacitors exhibited the remnant polarization of 18 μC/cm^2 and the dielectric constant as high as 1100.

Process Integration

A schematic fabrication process of the PAM is shown in Figure 11. On the front side of the silicon wafer coated with 2 μm-thick LPCVD low stress silicon nitride, 1500Å-thick platinum is deposited as the bottom electrode layer followed by deposition of 3600Å-thick PZT layer using sol-gel method. On top of the PZT, 1500Å-thick ruthenium oxide layer is deposited by reactive sputtering (a). RuO_2/PZT/Pt capacitor structure is patterned by self-aligned process using Cl_2/O_2 based plasma etching as in (b) and (c). After the gold mirror is delineated as in (d), silicon under the mirror plate and the cantilevers is removed by anisotropic etching in aqueous KOH (e). In this step, the front side of the wafer is passivated from the etchant by mechanical jigging. Finally, cantilevers and mirror plate are released by RIE

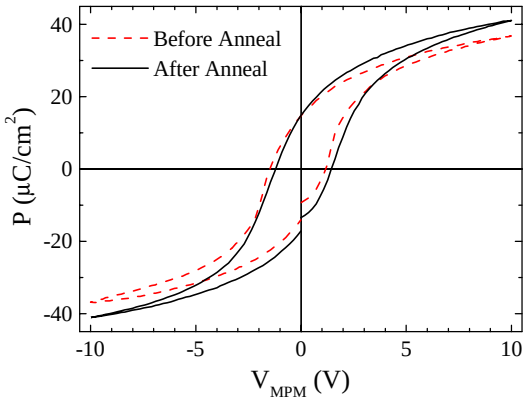

Figure 8: Polarization characteristics of the metal/PZT/metal capacitor with and without recover annealing after the dry etching steps.

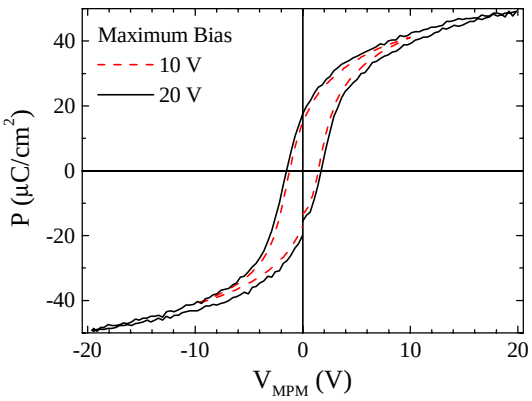

Figure 9: P-E curves of the 3600Å-thick PZT capacitor after recover annealing at 650 • .

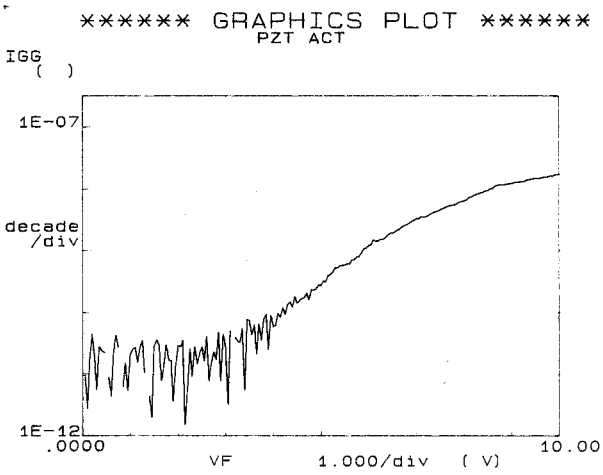

Figure 10. Leakage current characteristic of the RuO_2/PZT/Pt capacitor structure of PAM. Total area of the measured capacitor is about 1.5×10^6 μm^2.

from the front side of the wafer followed by dicing into individual chips (f). Figure 12 shows the fabricated PAM chip before packaging. The lateral dimension of the chip is 3 mm × 3 mm and the thickness is 525 μm, respectively. Slight upward bending was observed in the released PZT unimorph cantilevers due to the tensile residual stress of Pt and PZT films. The initial protrusion of the mirror plate from the silicon surface was measured about 5 μm in PAM with 250 × 250 μm^2 micromirror due to the bending of the cantilevers. This means that the stress gradient along the thickness direction of the PZT unimorph cantilevers is about 40 MPa/μm [8]. Most of the PAM with 1000 × 1000 μm^2 mirror plate was broken at the connection point of the hinge to the mirror plate after release process because the stress exerted on the connection hinges by the bending of the cantilevers exceeds the yield strength of the hinges as expected in numerical simulation. However, nearly all the PAMs having 500 × 500 μm^2 and 250 × 250 μm^2 were survived after the entire fabrication

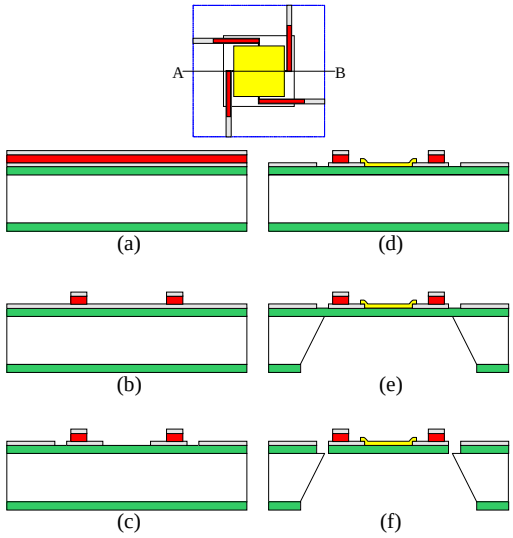

Figure 11: Fabrication process of the PZT actuated micromirror.

process. The PAM chips were mounted on the TO header stems and gold wires were bonded to each pad of the PAMs to measure the actuation characteristics of the PAM.

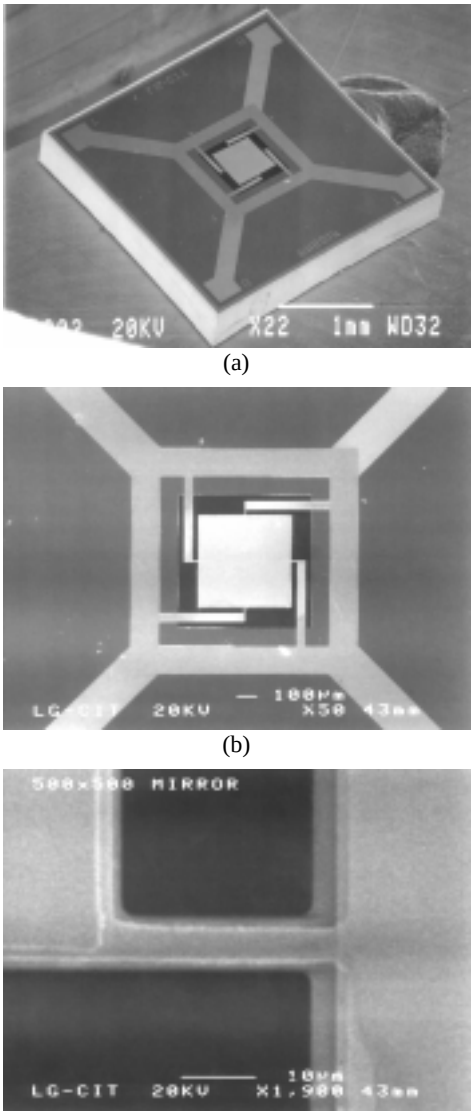

(a)

(b)

(c)

Figure 12: SEM images of the fabricated PAM with 500×500 μm^2 micromirror plate. (a) Entire chip. (b) Magnified image showing the micromirror. (c) Further magnification showing the hinge.

MEASUREMENT AND RESULTS

The out-of-plane vertical displacement of the micromirror of the PAM was measured by two different methods. One way is magnifying the displacement of the reflected laser spot by objective lens as in Figure 13(a). The other is use of interferometry with white light by calculating the changes in the fringe pattern according to the displacement of the mirror as in Figure 13 (b).

In the first measurement setup, He-Ne laser with 632.8 nm wavelength is used. The spot of the reflected laser beam from PAM on the focal point of first focusing lens is imaged on the pixels of the CCD camera by the objective lens. The magnified displacement of the laser spot incident on the CCD by the actuation of the PAM is captured by a frame grabber and calculated by counting the number of the pixels between the displaced beam image and the zero bias image. The distance between two adjacent pixels corresponds to 0.2 μm displacement of the micromirror and this is the resolution of the optical system in Figure 13(a). Minimum resolvable displacement was calibrated by stacked bulk PZT mirror whose displacement is well calibrated according to the applied voltage.

The second method depicted in Figure 13(b) utilizes white-light scanning interferometry and a commercial product Acura 1500F was used to measure the actuation characteristics of the PAM. It provided metrological information on the surface of the PAM. Figure 14 shows the fringe patterns at zero bias and 5 V DC bias applied to PAM, respectively. Even at the free standing condition, the micromirror deforms slightly in concave manner due to the residual tensile stress of the thin gold metal layer. The height difference between the highest and the lowest position in the mirror was 2.1 μm. However, the initial deformation of the mirror did not experience any considerable change during operation of the PAM as guaranteed in Figure 14. This result guarantees the parallel translational motion of the micromirror along the out-of-plane direction. To be used in the optics for the high-density optical data storage system, it is necessary to remove the mirror deformation. Figure 15 shows the actuated displacement *h* of the PAM with respect to the applied voltage. It shows that the micromirror moves more than 5 μm even under 10 V bias and it ensures the low voltage operation of the PAM. The micromirror moves upward along the dashed line with increasing voltage from the free standing position. Dashed line clearly shows the coercive field of the PZT

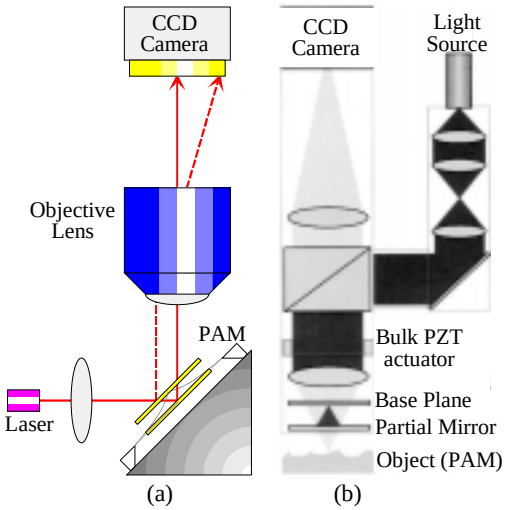

Figure 13: Two different optical setups to measure the displacement of the micromirror actuated by PZT unimorph cantilevers.

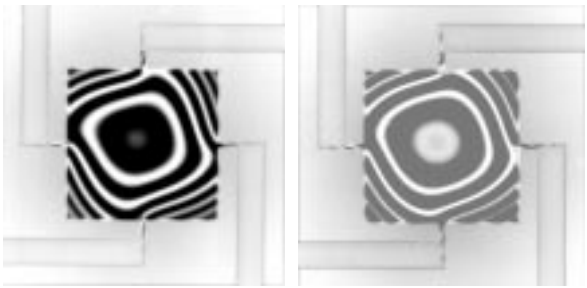

(a) (b)

Figure 14: Fringe patterns observed on the 250 × 250 μm^2 micromirror surface under no bias (a) and 5 V DC bias applied at the PZT cantilever actuators (b).

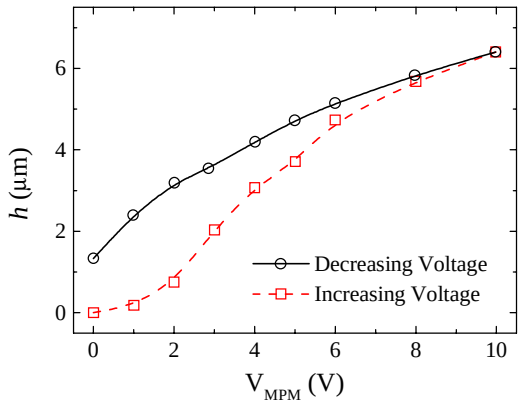

Figure 15: Actuation characteristic of PAM having 250 × 250 μm^2 micromirror.

unimorphs around 2 V. Once the positive voltage had been applied, the PAM was actuated along the solid line in this graph. Although the actuation characteristic shows saturation, the actuation resolution of the PAM around zero bias point is about 0.9 μm/V and the maximum non-linearity is 4% in the range of lower than 2 V.

CONCLUSION

In this work, the actuated micromirror (PAM) is proposed as a fine-tracking mechanism for the high-density optical data storage systems. A square shaped micromirror is actuated by the symmetrically arranged PZT unimorph cantilevers. The PAM is fabricated by the process integration of the conventional silicon micromachining technique and PZT sol-gel method. Even after the fabrication process, stacked PZT capacitor shows good properties in leakage current, breakdown, and polarization characteristics. The PAM can be operated under 5 V bias to steer the laser beam over 5 μm-stroke. The parallel motion of the micromirror along the out-of-plane direction is verified and any significant deformation of the mirror shape is not observed during operation. The resonant frequency of the PAM is expected to be high enough to satisfy the requirement of the servo bandwidth of the optical data storage with the data density of few tens Gbit/in^2. The initial shape of the micromirror is not perfectly flat and the cantilevers are bent upward in first fabrication result because of the residual stress in the stacked films. These undesirable factors should be suppressed through the optimization on the material selection and the process conditions through further work.

ACKNOWLEDGEMENTS

The authors would like to thank Mr. In-Seong Cho of LGCIT for his help on packaging the PAMs and Mr. T.-S. Kim of Intek Engineering Co. for his help on the optical measurements.

REFERENCES

[1] T. Hirano, L.-S. Fan, T. Semba, W. Y. Lee, and J. Hong, “Micro-actuator for tera-storage,” in *Proc. MEMS ‘99*, Orlando, FL, Jan. 1999, pp. 441-446.

[2] P. N. Minh, T. Ono, and M. Esashi, “A novel fabrication method of the tiny aperture tip on silicon cantilever for near field scanning optical microscopy,” in *Proc. MEMS ‘99*, Orlando, FL, Jan. 1999, pp. 360-365.

[3] L. P. Ghislain, V. B. Elings, K. B. Crozier, S. R. Manalis, S. C. Minne, K. Wilder, G. S. Kino, and C. F. Quate, “Near-field photolithography with a solid immersion lens,” *Appl. Phys. Lett.*, vol. 74. no. 4, Jan. pp. 501-503, 1999.

[4] G. S. Kino, “Optical background for near-field recording,” in *Proc. Magneto Optical Recording Int’l Sympo.*, Monterey, CA, Jan. 1999, pp. 1-6.

[5] S. Sumi, A. Takahashi, and T. Watanabe, “Advanced storage magnetooptical disk (AS-MO) system,” in *Proc. Magneto Optical Recording Int’l Sympo. ‘99*, Monterey, CA, Jan. 1999, pp. 173-176.

[6] D. A. Horsley, A. Singh, A. P. Pisano, and R. Horowitz, “Angular micropositioner for disk drives,” in *Proc. MEMS ‘97*, Nagoya, Japan, Jan. 1997, pp. 454-459.

[7] M. -H. Kiang, O. Solgaard, K. Y. Lau, and R. S. Muller, “Electrostatic combdrive-actuated micromirrors for laser-beam scanning and positioning,” *IEEE J. Microelectromech. Syst.*, vol. **7**, pp. 27-37, 1998.

[8] Y. Yee, M. Park, and K. Chun, “A sticking model of suspended polysilicon microstructure including residual stress gradient and postrelease temperature,” *IEEE J. Microelectromech. Syst*. vol. 7, no. 3, pp. 339-344, 1998.

[9] Y. Yee, Y.-S. Jeon, J. Bu, and G. Kim, “Integrated Multi-wavelength Laser Source Module with Micromachined Mirrors,” in *Proc. SPIE Micromachining and Microfabrication Conference*, Santa Clara, CA, Sep. 1999, pp. 398-406.

[10] D.-C. Kim, H.-J. Nam, W. Jo, H.-M. Lee, S.-M. Cho, J. Bu and H.-B. Kang, “Integration of a split word line ferroelectric memory using a novel etching technology,” *Integrated Ferroelectrics*, in press.